CVPR
JUNE 17-21, 2024
SEATTLE, WA

Rethinking Boundary Discontinuity Problem for Oriented Object Detection

Hang Xu[1,2*], Xinyuan Liu[2*] , Haonan Xu[2], Yike Ma[2], Zunjie Zhu[1], Chenggang Yan[1], Feng Dai[2†]

[1] Hangzhou Dianzi University, Hangzhou, China
[2] Institute of Computing Technology, Chinese Academy of Sciences, Beijing, China
[*]Equal contribution [†]Corresponding author

CONTENTS

1. Motivation

1.1 The Root of All Evil is “Box ≠ Object”

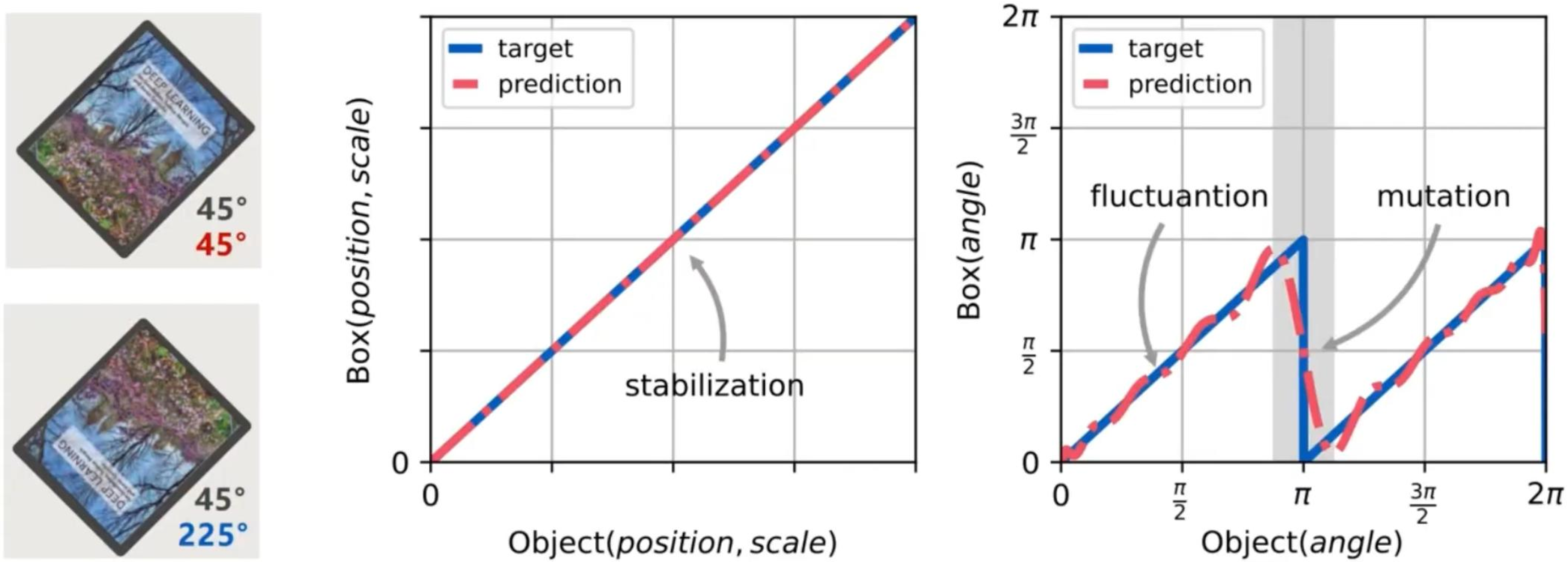

[CVPR 2024] Rethinking Boundary Discontinuity Problem for Oriented Object Detection

1.2 The Devil is in Encoding Mode

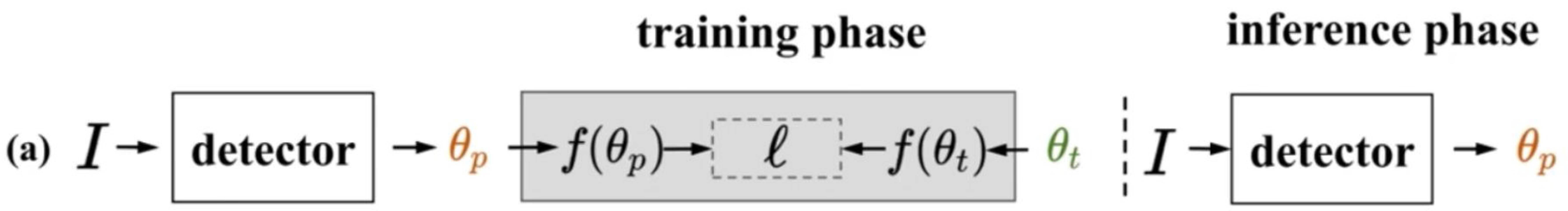

$$\theta = \arg\min_{\theta_p} \ell\big(f(\theta_p); f(\theta_t)\big) \rightarrow$$ **model fits discontinuous θ_p**

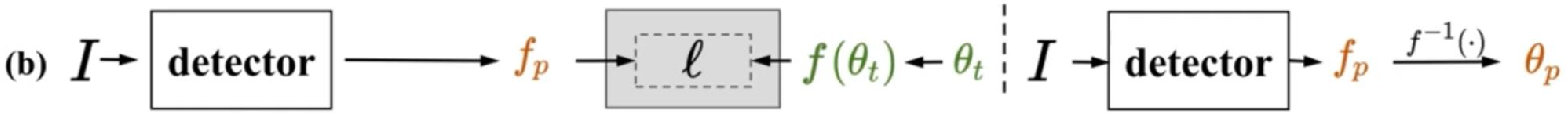

$$\theta = f^{-1}\Big(\arg\min_{f_p} \ell\big(f_p; f(\theta_t)\big)\Big) \rightarrow$$ **model fits continous f_p**

CVPR JUNE 17-21, 2024 SEATTLE, WA

2.1 Dual-Optimization Paradigm

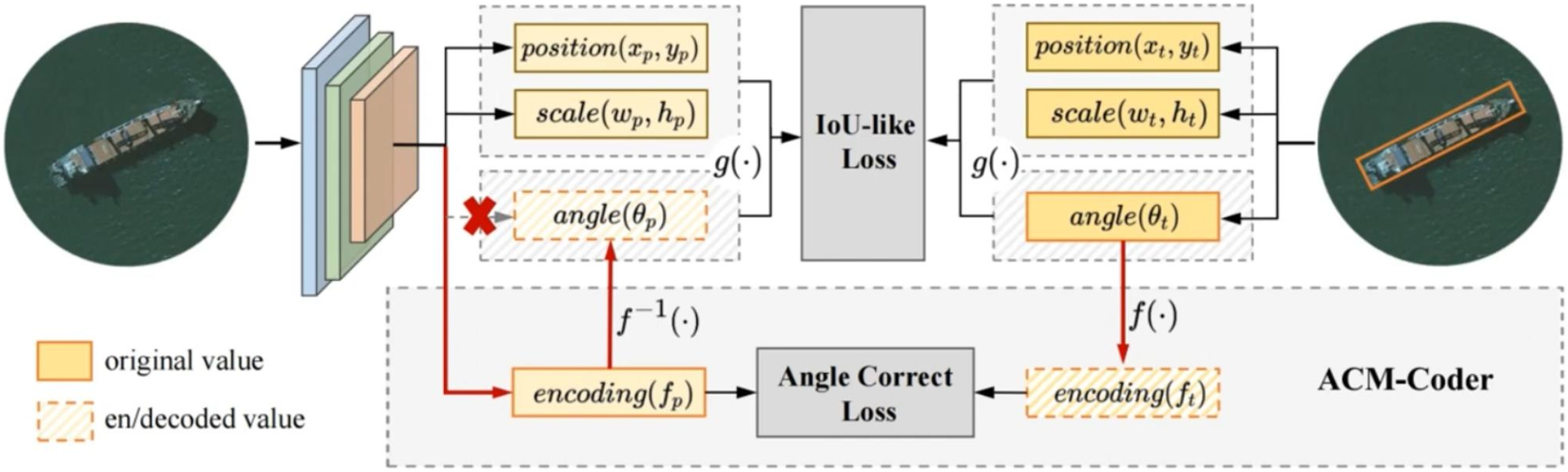

2.2 ACM-Coder

- $z = f(\theta) = e^{j\omega\theta}$
- $f_{box} = e^{i\omega\theta_{box}} = e^{i\omega(\theta_{obj} \bmod \pi)} = \begin{cases} e^{i\omega\theta_{obj}}, & \theta_{obj} \in [0, \pi) \\ e^{i\omega\theta_{obj}} \cdot e^{-i\omega\pi}, & \theta_{obj} \in [\pi, 2\pi) \end{cases}$

1) When $\omega = 1$, $e^{-i\omega\pi} = -1$, then

$$f_{box} = e^{i\omega\theta_{box}} = \begin{cases} e^{i\omega\theta_{obj}}, \theta_{obj} \in [0, \pi) \\ -e^{i\omega\theta_{obj}}, \theta_{obj} \in [\pi, 2\pi) \end{cases} = \begin{cases} f_{obj}, \theta_{obj} \in [0, \pi) \\ -f_{obj}, \theta_{obj} \in [\pi, 2\pi) \end{cases} = f_{obj} \cdot \text{sign}(\pi - \theta_{obj})$$

2) When $\omega = 2$, $e^{-i\omega\pi} = 1$, then

$$f_{box} = e^{i\omega\theta_{box}} = \begin{cases} e^{i\omega\theta_{obj}}, \theta_{obj} \in [0, \pi) \\ e^{i\omega\theta_{obj}}, \theta_{obj} \in [\pi, 2\pi) \end{cases} = f_{obj}$$

Thus, we select w=2 for ACM.

3.1 Comparison with the State-of-the-Art

Method	MS	PL	BD	BR	GTF	SV	LV	SH	TC	BC	ST	SBF	RA	HA	SP	HC	AP_{50}
PIoU		80.90	69.70	24.10	60.20	38.30	64.40	64.80	90.90	77.20	70.40	46.50	37.10	57.10	61.90	64.00	60.50
RoI-Trans.	✓	88.64	78.52	43.44	75.92	68.81	73.68	83.59	90.74	77.27	81.46	58.39	53.54	62.83	58.93	47.67	69.56
O^2-DNet	✓	89.31	82.14	47.33	61.21	71.32	74.03	78.62	90.76	82.23	81.36	60.93	60.17	58.21	66.98	61.03	71.04
DAL	✓	88.61	79.69	46.27	70.37	65.89	76.10	78.53	90.84	79.98	78.41	58.71	62.02	69.23	71.32	60.65	71.78
P-RSDet	✓	88.58	77.83	50.44	69.29	71.10	75.79	78.66	90.88	80.10	81.71	57.92	63.03	66.30	69.77	63.13	72.30
BBAVectors	✓	88.35	79.96	50.69	62.18	78.43	78.98	87.94	90.85	83.58	84.35	54.13	60.24	65.22	64.28	55.70	72.32
DRN	✓	89.71	82.34	47.22	64.10	76.22	74.43	85.84	90.57	86.18	84.89	57.65	61.93	69.30	69.63	58.48	73.23
CFC-Net	✓	89.08	80.41	52.41	70.02	76.28	78.11	87.21	90.89	84.47	85.64	60.51	61.52	67.82	68.02	50.09	73.50
Gliding Vertex		89.64	85.00	52.26	77.34	73.01	73.14	86.82	90.74	79.02	86.81	59.55	70.91	72.94	70.86	57.32	75.02
Mask OBB	✓	89.56	85.95	54.21	72.90	76.52	74.16	85.63	89.85	83.81	86.48	54.89	69.64	73.94	69.06	63.32	75.33
CenterMap	✓	89.83	84.41	54.60	70.25	77.66	78.32	87.19	90.66	84.89	85.27	56.46	69.23	74.13	71.56	66.06	76.03
CSL	✓	90.25	85.53	54.64	75.31	70.44	73.51	77.62	90.84	86.15	86.69	69.60	68.04	73.83	71.10	68.93	76.17
R^3Det	✓	89.80	83.77	48.11	66.77	78.76	83.27	87.84	90.82	85.38	85.51	65.67	62.68	67.53	78.56	72.62	76.47
GWD	✓	86.96	83.88	54.36	77.53	74.41	68.48	80.34	86.62	83.41	85.55	73.47	67.77	72.57	75.76	73.40	76.30
SCRDet++	✓	90.05	84.39	55.44	73.99	77.54	71.11	86.05	90.67	87.32	87.08	69.62	68.90	73.74	71.29	65.08	76.81
KFIoU	✓	89.46	85.72	54.94	80.37	77.16	69.23	80.90	90.79	87.79	86.13	73.32	68.11	75.23	71.61	69.49	77.35
DCL	✓	89.26	83.60	53.54	72.76	79.04	82.56	87.31	90.67	86.59	86.98	67.49	66.88	73.29	70.56	69.99	77.37
RIDet	✓	89.31	80.77	54.07	76.38	79.81	81.99	89.13	90.72	83.58	87.22	64.42	67.56	78.08	79.17	62.07	77.62
PSC	✓	89.86	86.02	54.94	62.02	81.90	85.48	88.39	90.73	86.90	88.82	63.94	69.19	76.84	82.75	63.24	78.07
KLD	✓	88.91	85.23	53.64	81.23	78.20	76.99	84.58	89.50	86.84	86.38	71.69	68.06	75.95	72.23	75.42	78.32
CenterNet-ACM	✓	89.84	85.50	53.84	74.78	80.77	82.81	88.92	90.82	87.18	86.53	64.09	66.27	77.51	79.62	69.57	**78.53**
RoI-Trans.-ACM	✓	85.55	80.53	61.21	75.40	80.35	85.60	88.32	89.88	87.13	87.10	68.15	67.94	78.75	79.82	75.96	**79.45**

3.2 Ablation Study

Method	HRSC2016 (Ship)		UCAS-AOD (Car)		UCAS-AOD (Plane)		DOTA-v1.0	
	AP_{50}	AP_{75}	AP_{50}	AP_{75}	AP_{50}	AP_{75}	AP_{50}	AP_{75}
GWD	84.94	61.87	87.25	28.46	90.34	38.22	73.12	34.98
ACM-GWD	90.63 (+5.69)	86.71 (+24.84)	88.69 (+1.44)	29.15 (+0.69)	90.35 (+0.01)	76.00 (+37.78)	73.71 (+0.59)	41.97 (+6.99)
KLD	90.01	79.29	87.54	29.99	90.33	29.19	73.41	35.25
ACM-KLD	90.55 (+0.54)	87.45 (+8.16)	88.76 (+1.22)	30.40 (+0.41)	90.39 (+0.06)	75.65 (+46.46)	73.95 (+0.54)	42.97 (+7.72)
KFIoU	88.26	62.95	85.74	24.44	90.34	16.81	71.97	26.11
ACM-KFIoU	90.55 (+2.29)	87.77 (+24.82)	88.31 (+2.57)	34.81 (+10.37)	90.40 (+0.06)	74.48 (+57.67)	74.51 (+2.54)	40.49 (+14.38)
SkewIoU	89.39	76.43	87.73	27.59	90.34	63.64	73.62	38.01
ACM-SkewIoU	90.47 (+1.08)	88.33 (+11.09)	88.27 (+0.54)	29.13 (+1.74)	90.37 (+0.03)	75.13 (+11.49)	74.21 (+0.59)	42.83 (+4.37)

Typical IoU-like methods are improved to the same level, indicating that the primary distinction between them lies in their optimization capabilities for the angular boundary.

3. Experiment

3.3 Visualized Results

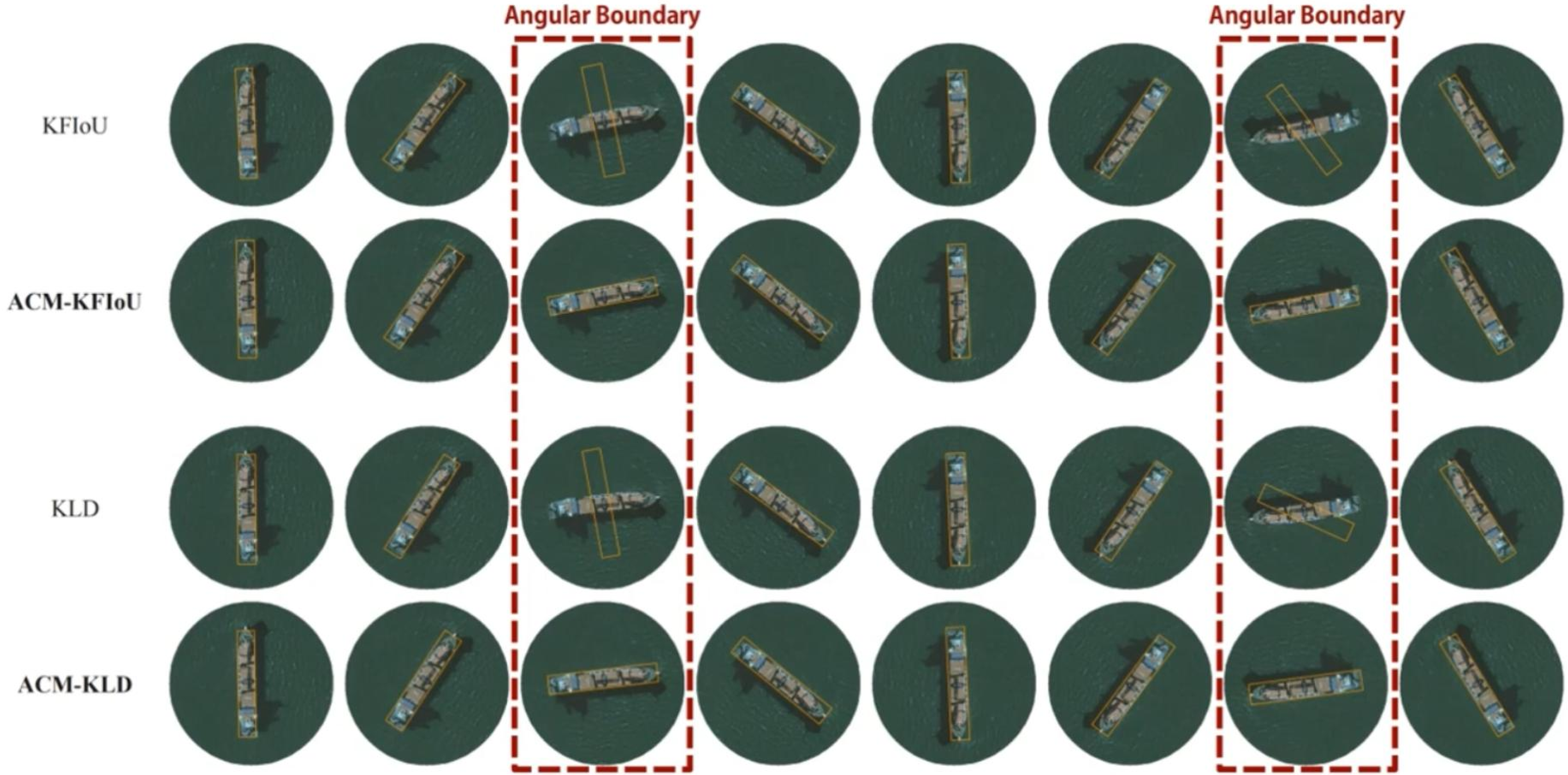

CVPR
JUNE 17-21, 2024
SEATTLE, WA

Rethinking Boundary Discontinuity Problem for Oriented Object Detection

Hang Xu[1,2*], Xinyuan Liu[2*] , Haonan Xu[2], Yike Ma[2], Zunjie Zhu[1], Chenggang Yan[1], Feng Dai[2†]

[1] Hangzhou Dianzi University, Hangzhou, China
[2] Institute of Computing Technology, Chinese Academy of Sciences, Beijing, China
[*]Equal contribution [†]Corresponding author

Any questions please contact us!